

<https://doi.org/10.1038/s43247-024-01362-2>

Deep-living and diverse Antarctic seaweeds as potentially important contributors to global carbon fixation

Check for updates

Leigh W. Tait^{1,2}✉, Caroline Chin³, Wendy Nelson^{4,5}, Steve George¹, Peter Marriott³, Richard L. O'Driscoll³, Miles Lamare⁶, Victoria S. Mills³ & Vonda J. Cummings³

Global models predict that Antarctica has little suitable habitat for macroalgae and that Antarctic macroalgae therefore make a negligible contribution to global carbon fixation. However, coastal surveys are rare at southern polar latitudes (beyond 71° S), and here we report diverse and abundant macroalgal assemblages in un-navigated coastal habitats of the Ross Sea from 71.5°–74.5° S. We found extensive macroalgal assemblages living at depths >70 m and specimens of crustose coralline algae as deep as 125 m. Using global light modelling and published photosynthetic rates we estimate that Antarctic macroalgae may contribute between 0.9–2.8 % of global macroalgal carbon fixation. Combined, this suggests that Antarctic macroalgae may be a greater contributor to global carbon fixation and possibly sequestration than previously thought. The vulnerability of these coastal environments to climate change, especially shifting sea ice extent and persistence, could influence Southern Ocean carbon fixation and rates of long-term sequestration.

Macroalgae are increasingly recognised for their value in contributing to global carbon sequestration or Blue Carbon^{1–5}. Transport of seaweed biomass to subtidal sediments can result in up to 10% of that biomass becoming buried and locked away from the atmosphere⁶, with cold polar environments likely to encourage greater rates of sequestration⁷. Efforts to quantify Arctic macroalgal blue carbon suggest that their carbon sequestered is globally significant^{7–10}, but there is little information on the contribution of Antarctic seaweeds^{5,11–14}.

Global models predict that the Antarctic has very little suitable habitat for marine macroalgae¹⁵. Large-brown macroalgae provide key ecological functions such as habitat provision and are the dominant contributor to global macroalgal primary productivity¹⁵. However, observations of Antarctic macroalgae are sparse and largely limited to regions such as the Antarctic Peninsula^{16,17}. In these areas, however, macroalgae can reach standing biomass of between 0.25 and 1 kg (dry weight (DW) per m²^{18–20}), greater than some estimates of Arctic ecosystems (0.17–0.8 kg DW m⁻²^{21,22}), and comparable to some temperate ecosystems (0.4–4.5 kg DW m⁻²^{23–25}). These macroalgae provide key habitat for microalgae, invertebrates, and fish^{26–28}, are important drivers of benthic foodwebs through detrital subsidies^{29,30}, and may contribute significantly to carbon sequestration^{1,11}.

High rates of macroalgal material delivered to deep water in the Antarctic (>2000 m³) indicate that Antarctic macroalgae meet key criteria for long-term carbon sequestration¹.

Greenhouse gas emissions and the associated atmospheric and oceanic warming are causing unprecedented glacial retreat^{32,33} and dramatic changes in sea-ice extent^{33–35}. Glacial retreat and the associated increases in meltwater and delivery of sediments to coastal environments are rapidly changing the land–sea dynamics of the Antarctic continent with both positive and negative implications for macroalgal carbon sequestration^{14,36,37}. Likewise, sea ice concentration is strongly negatively correlated with macroalgal cover and projected future sea ice loss could increase overall macroalgal cover³⁸. Gains in blue carbon associated with increasing availability of suitable habitat following glacial retreat^{39–42} may be offset by increasing benthic disturbance from ice bergs^{43,44}. Identifying the spatial and vertical distribution of Antarctic macroalgae is critical in assessing how carbon sequestration pathways are being affected by climate-driven glacial retreat and sea-ice loss.

Light availability at the seafloor is a fundamental physiological limitation that determines both the latitudinal and depth ranges occupied by benthic macroalgae⁴⁵. Climate-driven shifts in suspended sediments and

¹National Institute of Water and Atmospheric Research, 10 Kyle St, Riccarton, Christchurch 8011, New Zealand. ²University of Canterbury, Private Bag 4800, Christchurch 8140, New Zealand. ³National Institute of Water and Atmospheric Research, 301 Evans Bay Parade, Hataitai, Wellington 6021, New Zealand.

⁴University of Auckland, 5 Symonds St, Auckland Central, Auckland 1010, New Zealand. ⁵Tamaki Paenga Hira Auckland War Memorial Museum, Parnell, Auckland 1010, New Zealand. ⁶Department of Marine Science, University of Otago, 310 Castle Street, Dunedin 9016, New Zealand. ✉e-mail: leigh.tait@niwa.co.nz

phytoplankton could increase the attenuation of light through the water column^{45,46}, and reduce the depth thresholds of benthic macroalgae⁴⁷. Despite the challenges for light harvesting at polar regions, thriving populations of benthic algae (particularly rhodophytes and phaeophytes) are found at depths below 40–60 m in both Arctic and Antarctic locations^{17,48}, with reports of phaeophytes (i.e., *Himantothallus grandifolius* (A.Gepp & E.S.Gepp) Zinova) at South Georgia as deep as 70 m¹⁷. As exploration of Antarctic benthic ecosystems increases, records of deep-living algae are increasingly being reported (e.g., red alga *Palmaria decipiens* found at ca. 100 m⁴⁹).

Adaptation to low light intensities is a key attribute of Antarctic macroalgae^{50–52}, but there are few verifiable records of large canopy-forming brown algae beyond the Antarctic Peninsula¹⁶. The southernmost observed populations of the large brown algae *H. grandifolius* were found at 72°25'S in the Ross Sea in 1966^{53,54} and during explorations at Cape Hallett at 20 m depth in 2004^{25–28}. Therefore, the current paradigm is that canopy-forming brown macroalgae and macroalgae, in general, are greatly limited in both their southern distribution¹⁶ and their habitable depth range in Antarctica.

Results and discussion

Here, we report dense populations of attached canopy-forming brown algae (Phaeophyceae *H. grandifolius*) at up to 74–95 m depth at multiple locations on the northern Victoria Land Coast in the Ross Sea, Antarctica; Robertson Bay, Cape Adare, Possession Islands, Cape Hallett. At several stations, including a transect completed at 70–74 m depth at the Possession Islands in 2021 (Fig. 1a), dense populations of large, attached specimens with fronds up to ca. 3 m length were identified (Fig. 1b, c) as well as dense populations of fleshy red algae, and Crustose Coralline Algae (CCA) (Fig. 1d). These observations align with previous records from South Georgia region where *H. grandifolius* was identified by remotely operated vehicles¹⁶. Alongside these observations, a diverse range of rhodophytes (red algae), chlorophytes (green algae), and phaeophytes (brown algae) were observed across transects at multiple stations. Samples were taken at several locations, including herbarium voucher specimens (see Supplementary Fig. 1 and Supplementary Tables 1–4). A maximum of 14 potential species were found at 50–70 m depths (Supplementary Table 4), representing diverse deep-living macroalgal assemblages, even when compared to temperate regions⁵⁹.

Several distinct macroalgal taxonomic groups were identified across the northern Victoria Land Coast, including rhodophytes (red algae), chlorophytes (green algae), and phaeophytes (brown algae) (Fig. 2a, Supplementary Fig. 1, Supplementary Tables 1–4⁶⁰). *H. grandifolius* was found as far south as Cape Hallett (72.2°S) but did not extend to Wood Bay (74.5°S) and has not, to our knowledge, been observed previously at intermediate latitudes. Observations of macroalgae across depths revealed that rhodophytes were found as deep as 99 m, CCA at 125 m, and *Desmarestia menziesii* J.Agardh and *H. grandifolius* were observed between depths of 75–95 m (Fig. 2b). Additionally, the green alga *Monostroma hariotii* Gain, red algae *Ballia* sp., *Iridaea* sp., *Palmaria* sp., *Phycodryis antarctica* (Skottsb.) Skottsb., *Plocamium* sp., CCA, possible *Rhodomenia*, and five yet-to-be-identified red algal species were lodged as herbarium specimens (Supplementary Table 4).

Drift algae from several taxonomic groups (e.g., brown algae, green algae, and red algae) were common at depths beyond 100 m, including several incidences of *H. grandifolius* at depths greater than 200 m. The high frequency of apparent drift algae at a range of depths made it difficult to reconcile the true habitable range of macroalgae in Antarctica but suggests that transport rates to deeper water may be high, as corroborated by previous sampling in the region^{55,56}.

The presence of deep-living macroalgal populations and the high incidence of drift algae required the examination of potential light budgets at these depths for the Antarctic region. To explore this, we used modelled estimates of light at the seabed (EBed⁴⁶) to (1) understand the likelihood that these populations are a persistent feature (i.e., is the modelled available light consistent with known limits); and (2) re-assess estimates of the possible regional distribution and carbon fixation of Antarctic macroalgae. We utilised the global modelling of Gattuso et al. (2020)⁴⁶, which estimates annual Photosynthetically Active Radiation (PAR) at the ocean surface and couples this with global bathymetric layers and estimates of light attenuation through the water column to derive EBed.

Global seafloor light⁴⁶ showed that light intensities at our surveyed locations and depths were in some cases $>0.1 \text{ mol m}^{-2} \text{ day}^{-1}$ (Fig. 3a), sufficient for photosynthesis. However, there were frequent observations of light intensities $<0.01 \text{ mol m}^{-2} \text{ day}^{-1}$ at the surveyed depths and latitudes (Fig. 3b), below expected thresholds for most macroalgae⁴⁶. We expect that

Fig. 1 | Multi-beam echosounder (MBES) map of the seafloor bathymetry near the Possession Islands, Ross Sea and associated seafloor imagery of macroalgal assemblages. Each station surveyed in 2021 and 2023 is shown by circles overlaid MBES imagery and on Landsat (USGS) satellite imagery (a), including the first station where large macroalgae were detected in 2021 (as indicated by white arrow). Orthoimage of the benthos at this station shows dense macroalgal assemblages on the seafloor (b), including dense stands of *H. grandifolius* (c), Crustose Coralline Algae (CCA), and fleshy red algae (d). The partial seafloor transect pictured in (b) ranges in depth from 70 to 74 m.

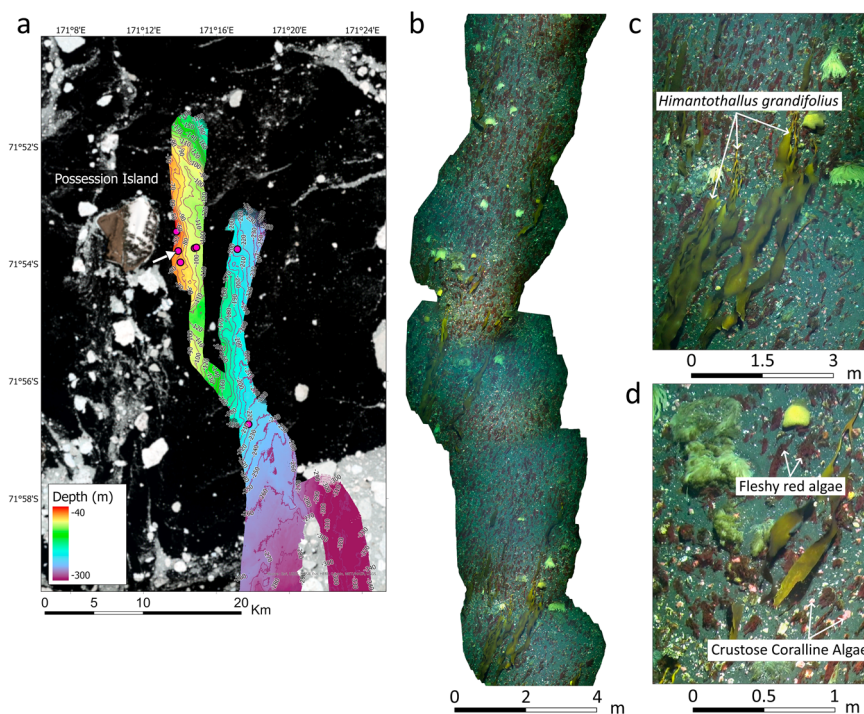


Fig. 2 | Presence, abundance, and depth distribution of several functional groups of macroalgae across stations (red dots) in the Ross Sea, Antarctica. Available global bathymetric data are presented and bounded between 0–200 m depth (a). Pie charts (a) show the presence of macroalgal functional groups at each location (numbered 1–5 for Robertson Bay, Cape Adare, Possession Islands, Cape Hallet and Wood Bay, respectively). The depth distribution of each macroalgal group across all stations (b) shows the density of individual thalli for each transect ($\pm 95\%$ CI). Note the y-axes are square root transformed to visualise transects where very low densities were recorded. Depth and density data are fitted using general additive models (GAM).

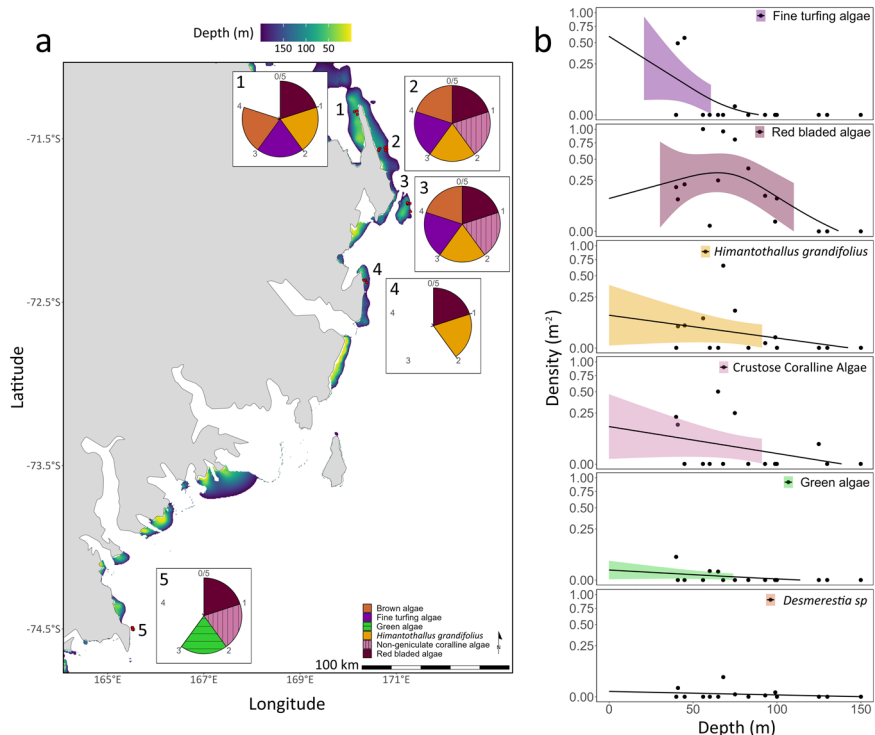
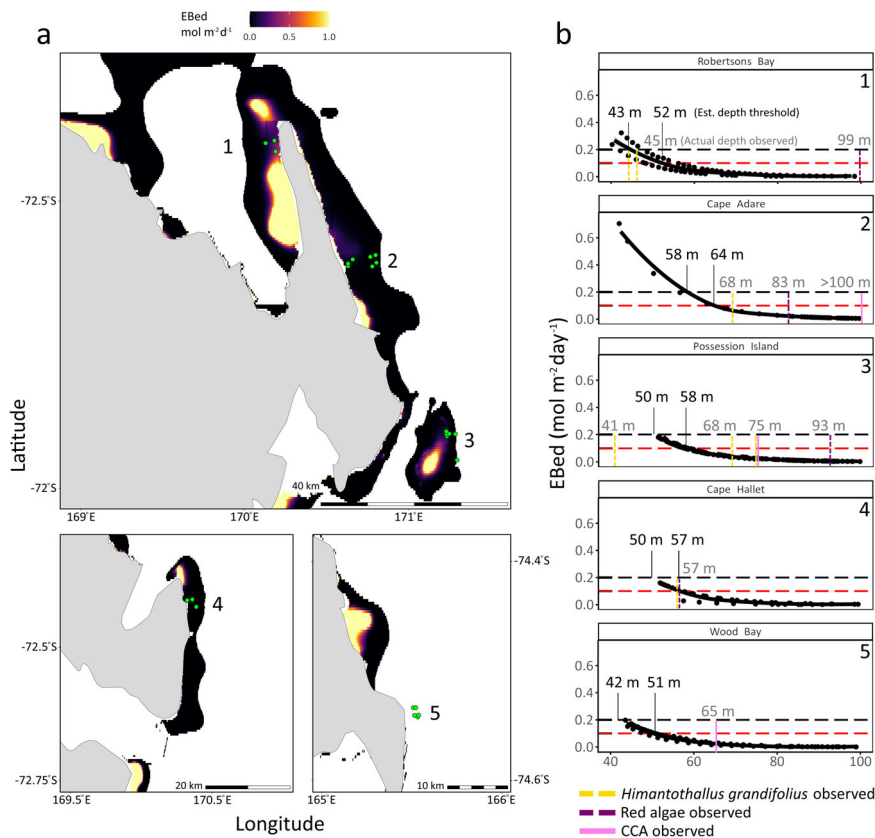


Fig. 3 | Seabed light availability ($\pm 95\%$ CI) for the coastal Ross Sea (EBed $\text{mol m}^{-2} \text{day}^{-1}$) as identified with global bathymetric layers, annual surface light budgets, and water clarity estimates. Seabed light availability (EBed) is shown across the five regions where benthic imagery was collected, with the green points showing the locations of benthic surveys performed in 2021 and 2023 (a). EBed across depths is reported for the five surveyed regions (1–5), averaged over three transects (across depth gradients, perpendicular to shore; b). The depths at which light falls below two thresholds (0.1 and $0.2 \text{ mol m}^{-2} \text{day}^{-1}$; indicated by black and red dashed horizontal lines, respectively) were reported for each region (vertical solid black lines), as well as the depths at which clearly attached populations of *H. grandifolius*, red algae, and crustose coralline algae (CCA) were observed (vertical dashed lines). Note that the bathymetry at some sites (i.e., Wood Bay, 5) was not resolved by global products and therefore is missed from global models (e.g. ref. ¹⁴).



three key mechanisms are responsible for these observations: (1) Antarctic macroalgae are remarkably adapted to low light intensities^{50–52}, (2) transport of macroalgae to deeper water, even while still attached to substrata, frequently occurs in Antarctica, and (3) estimates of light at the seabed may be less than realised EBed during certain critical periods.

We used literature-derived photosynthetic parameters to examine the physiological capabilities and possible depth thresholds of three common Antarctic macroalgae by extrapolating EBed across modelled values throughout ice-free regions of the Ross Sea. The results indicate that the red algal species *P. decipiens* (Fig. 4a) has potential net carbon gains at depths

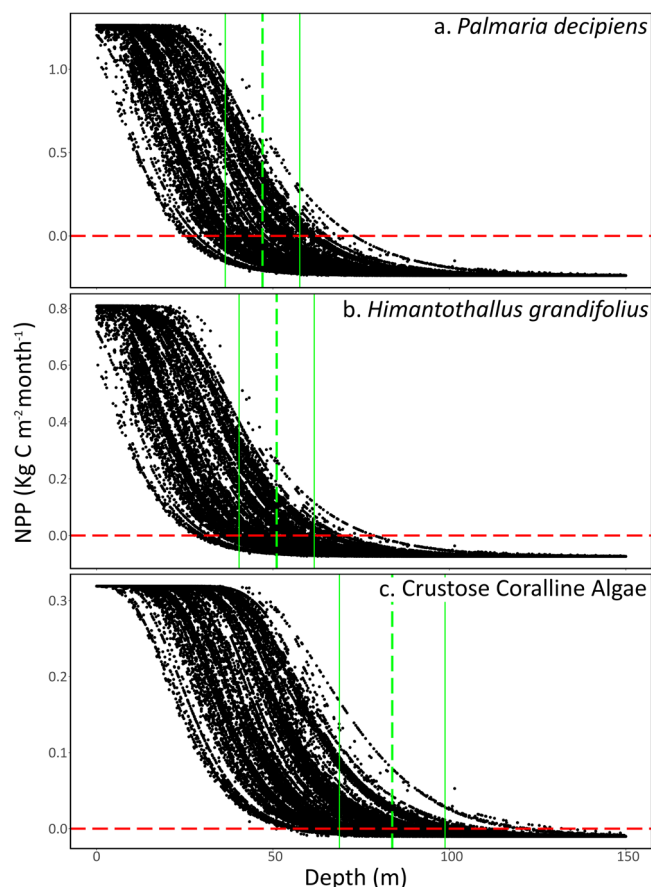


Fig. 4 | Net primary productivity (NPP) of three species (*P. decipiens*), (*H. grandifolius*), (*Crustose Coralline Algae*) against depth for every tile (1/4 degree) of seafloor that has estimated light at the seabed (EBed) for depths between 0 and 200 m (Gattuso et al., 2020⁴⁶). Light at the seabed for every tile was converted to net primary production (NPP) using literature-derived photosynthetic parameters (*P. decipiens*, a; *H. grandifolius*, b; Gomez et al. 1997⁵⁰; CCA, c; Schwarz et al. 2005⁵¹). The red horizontal line shows the “compensation point” of each seaweed, the point at which photosynthesis and respiration are balanced. Points below this line show net carbon loss, while points above show net carbon gain. The vertical green dashed line shows the mean depth at which the compensation point is crossed, and the solid green lines are one SD from the mean.

Table 1 | Estimated annual carbon fixation for three model species, *H. grandifolius*, *P. decipiens*, and CCA using published photosynthetic parameters^{48–50} and modelled seafloor light across the Ross Sea and entire Antarctic region (Gattuso et al., 2020⁴⁴)

| Species | Carbon fixed (Tg yr ⁻¹) | | Percentage of global carbon fixed by macroalgae | |
|------------------------|-------------------------------------|------------|---|------------|
| | Ross Sea | Antarctica | Ross Sea | Antarctica |
| <i>H. grandifolius</i> | 0.2–1.0 | 3–14 | 0.02–0.08 | 0.3–1.1 |
| <i>P. decipiens</i> | 0.6–1.2 | 7.5–15 | 0.05–0.09 | 0.6–1.2 |
| CCA | 0.1–0.5 | 1.3–7.9 | 0.008–0.03 | 0.1–0.6 |
| Total | 1–2.7 | 12–37 | 0.07–0.2 | 0.9–2.8 |

Fixed carbon is specified as Terra grams carbon fixed per annum and as a percentage of estimated annual global macroalgal carbon fixation (see Duarte et al., 2022¹⁴).

between 0 and 70 m (mean = 45 m), *H. grandifolius* (Fig. 4b) to ~75 m (mean = 50 m), and CCA (Fig. 4c) as deep as 125 m (mean = 80 m). While results showed some alignment with our observations of macroalgal maximum depths (i.e., 75 and 125 m for *H. grandifolius* and CCA, respectively),

we note that occurrences of red algae were seemingly beyond the edge of physiological capabilities for light harvesting according to modelled Ebed, and greater than expected from physiological modelling of *P. decipiens*. Compared to the global summary of macroalgal NPP, the NPP rates reported here were comparable to some temperate and many tropical and subtropical estimates⁶¹.

Combined, our observations and modelling corroborate the evidence that Antarctic algae are physiologically well adapted to low irradiance^{50–52} (Fig. 4) and may also experience high rates of dislodgement and transport to deeper waters³¹. While it is difficult to assess the accuracy of modelled seafloor light estimates without long-term in situ measurements, it is likely that modelled Ebed is higher than realised light on account of the variability of atmospheric and oceanographic processes affecting the intensity and attenuation of light through the water column⁴⁶. We note that consolidated sea-ice and drifting sea-ice floes likely represent a consistent feature across many of the regions surveyed here, with significant implications for the delivery of light to the seafloor. Despite these challenges, dense assemblages of multiple functional groups of Antarctic macroalgae were found at depths with expected light intensities near the limits for photosynthetic organisms.

We used the observed latitudinal ranges and densities of the three modelled species/functional groups to extrapolate carbon fixation across the Ross Sea and the entire Antarctic region. Estimates of the potential contribution of macroalgal productivity were based on photosynthetic parameters (i.e., Fig. 4^{51,52}) and modelled seabed light for each cell of bathymetric data⁴⁶. These calculations showed that these three species may fix a combined total of 2.7 Tg across the Ross Sea and 37 Tg across Antarctica (Table 1). Shallow water studies (e.g., <20 m) in the Antarctic Peninsula region estimate 0.25 Tg carbon per year¹⁴, while we estimate that NPP by *H. grandifolius* alone is likely to be more than 0.2 Tg carbon per year in the Ross Sea. When compared to global estimates of annual carbon fixation by macroalgae, Antarctic macroalgae have the potential to contribute up to 2.8% of the global budget¹⁵, with *H. grandifolius* and *P. decipiens* possibly contributing 1.1% and 1.2%, respectively (Table 1).

Here, we report some of the deepest verified records of macroalgae in the Antarctic polar region, including dense populations of the large brown alga *H. grandifolius*. This coincides with increasing numbers of deep observations of Antarctic seaweeds^{16,49} and unprecedented declines in Antarctic sea-ice cover in recent years^{34–36,62}. Using global seabed light products⁴⁶ and photosynthetic parameters of several Antarctic seaweed species^{50–52}, we examine the full profile of light attenuation scenarios in the Ross Sea and show that observed distributions are in line with but in some cases beyond, the expected limits of physiological light requirements. From our observations of specimens inhabiting depths between 40 and 125 m, we conclude that Antarctic macroalgae may be more abundant than global models suggest¹⁵, are transported at high rates to the deep ocean where sequestration can occur and are therefore possibly poorly represented in estimates of global benthic primary productivity^{14,41}.

To our knowledge, there are not yet any direct observations of large brown macroalgae at depths beyond 20 m near their southern limits (e.g., 72°S in the Ross Sea), although there are direct observations from the Antarctic Peninsula (e.g., 60–65°S) of populations at 50–70 m depth^{17,27}, which fits well with physiological studies of minimum light requirements^{63,64}. There are, however, deeper records (e.g., 70–100 m) of unverified dredged material from locations including the Antarctic Peninsula⁶⁵ and the Ross Sea region as far south as 73°S^{55,66}. Recent studies using remotely operated vehicles (ROV) have verified rhodophytes as deep as 100 m in the Antarctic Peninsula region⁴⁹. Similarly, Arctic kelps have increasingly been found penetrating deeper waters^{67,68}, including as deep as 61 m at 67°N⁶⁹ and red algae as deep as 68 m at 78°N⁷⁰.

These discoveries are of significance to global estimates of carbon fixation and potential sequestration by benthic macroalgae. Contemporary paradigms suggest that Antarctica has minimal coverage of benthic photoautotrophs and that shallow benthic habitats receive little annual solar radiation on account of sea-ice cover for long periods and low solar angles⁷¹. However, numerous studies, particularly from the West Antarctic Peninsula

region and the South Shetland Islands, show abundant and rich assemblages of macroalgae^{72–74}. This study extends the projection of abundant macroalgal assemblages into higher Antarctic latitudes and greater depths.

The Southern Ocean is a key carbon sink⁷⁵, and while phytoplankton undoubtedly drive CO₂ uptake^{76,77}, the role of macroalgae may be underestimated. Our results identify both significant coverages of attached large macroalgae in relatively deep waters (e.g., 60–125 m) but also numerous observations of drift algae in deep water (e.g., >200 m) and in previous studies⁵⁵. Extension of macroalgal populations into deeper areas and the apparent high densities of attached and drift algae beyond 100–200 m support the assertion that macroalgal carbon export and sequestration is potentially significant in the Antarctic region^{11,14,41}.

Newly ice-free areas in the Antarctic Peninsula have been followed by rapid colonisation by benthic macroalgae with substantial gains in carbon standing stock and possibly carbon sequestration⁴². However, increased meltwater input (and associated sediment or nutrient run-off), rising temperatures, reductions in sea-ice cover, and alterations in the timing and abundance of phytoplankton blooms have implications for light attenuation and, therefore, the habitable depth range of benthic macroalgae^{39–42}. While reductions in sea-ice cover may increase the amount of light penetrating through the often remarkably clear surface waters to the seafloor^{61,70,78}, earlier onset of phytoplankton blooms may offset these gains, especially at greater depths⁴⁷.

These findings shed light on the Antarctic coastal region as a potentially important habitat for benthic macroalgae. Our voyages targeted uncharted, shallow coastal waters of the Ross Sea region and identified widespread, dense macroalgal beds and a high abundance of drift algae. Negligible contribution of Antarctic seaweed carbon fixation in global models¹⁵ is likely a result of poor survey coverage and limited verified bathymetry (a key requirement for habitat suitability modelling) for the Antarctic coastal marine area. Improving our understanding of the realised light environment, macroalgal biomass, and the fate of macroalgae will be essential in uncovering the role of Antarctic macroalgae in global carbon budgeting and the possibility of positive feedback loops with recent unprecedented and record-breaking sea-ice minima^{34–36,62}. Quantifying these processes in the context of the Ross Sea Marine Protected Area⁷⁹ will be essential in providing guidance for the ongoing management of ecosystem services, especially where bottom contact disturbances may alter long-term carbon storage⁸⁰. These discoveries and the associated carbon sequestration potential provide important evidence for the continued preservation and protection of Antarctic benthic areas, particularly for poorly understood macroalgal habitats⁸¹.

This research provides impetus to better understand the dynamics of benthic communities in the photic and mesophotic zone of the Antarctic region, the potential consequences of altered glacial and sea-ice dynamics, and to uncover the possible contributions of and trajectories for polar carbon sequestration.

Methods

In January and February 2021 and 2023, the New Zealand National Institute of Water and Atmospheric (NIWA) research vessel *Tangaroa* travelled to the Ross Sea region, focussing on coastal regions of northern Victoria Land, Ross Sea, Antarctica, spanning Robertson Bay (west of Cape Adare) to Terra Nova Bay (ca. 71°–75° latitude). Benthic surveys with towed and remote-operated camera systems were completed at five locations (25 individual sampling stations) at depths between 40 and 250 m.

Benthic surveys

Un-navigated regions of the Ross Sea were mapped using RV *Tangaroa*'s Kongsberg EM302 multibeam echosounder (MBES) to survey coastal benthic habitats as shallow as 40 m. Once suitable areas were covered by MBES, remote seafloor imaging using a Deep-Towed Imaging System (DTIS) was carried out across 200–500 m long transects parallel to the shore. Although specific depth strata were targeted, the presence and movement of sea-ice affected the exact deployment depths at many sites.

In total, five ice-free locations from Robertson Bay to Terra Nova Bay were sampled.

DTIS is a battery-powered towed camera frame, which records continuous high-definition digital video (1080 p, Sony HDR PJ 760VE) and simultaneously takes high definition still images (24 megapixel Nikon D3200) at 10 s intervals⁸². The video camera faces forward at about 35° from vertical and the still camera faces directly downwards (0°). Full resolution video and still images are recorded at the seabed and downloaded on return to the surface. A lower-resolution video image is transmitted to the surface in real-time enabling control of camera altitude and initial evaluation of seabed substratum types and biological assemblages. DTIS transects were at a target altitude above the seabed of 2.0–3.5 m. The seabed position and depth of DTIS were tracked in real-time using the SIMRAD HiPAP system. Parallel lasers mounted on the towed platform allowed for scaling of seafloor images and video.

The seabed position of DTIS was plotted in real time using OFOP software (Ocean Floor Observation Protocol, www.ofop-by-sams.eu). All navigation data, camera commands, and spatially referenced observations of seabed type and the occurrence of biological assemblages were recorded to OFOP log files and captured by the ship's Data Acquisition System (DAS). A Seabird Micocat CTD was attached to the DTIS frame during all deployments to record salinity, temperature, and depth data.

Imagery processing and analysis

Video imagery collected by the DTIS system was processed by taxonomists. All macroalgal specimens clearly attached to the seafloor were identified during processing. Macroalgal species were identified to the highest taxonomic level possible using key morphological features from the video, the higher resolution still images, and, where available, via the collection of physical specimens. For the assignment and annotation of the functional groups, taxonomists and parataxonomists first scored these groups using modern taxonomic labels where possible. If it was not possible to identify the macroalgal groups to the taxonomic level and/or to confirm identifications with taxonomists, we reverted to using a similar scoring methodology to the Collaborative and Automated Tools for Analysis of Marine Imagery (CATAMI) scheme that combines coarse-level taxonomy and morphology⁸³. However, the CATAMI vocabulary can be convoluted and ambiguous, so we have simplified the vocabulary for some of the functional groups⁸⁴.

Density of each taxonomic group was calculated by dividing abundance by the total area of the transect (calculated using transect length and width). Transect width was calculated using the scaling lasers to estimate frame coverage at multiple points along the transect.

The presence of unattached drift algae was common across all stations, including at two stations that were greater than 200 m deep (Possession Islands). Stations where clearly attached specimens were observed, were noted separately from sites with infrequent and un-attached specimens. Some stations where very low densities of apparently attached macroalgae were further assessed using light and metabolic modelling to help determine the likelihood that these specimens were dislodged drift algae or capable of inhabiting the observed depths/latitudes.

Individual stations were processed into ortho-mosaic imagery to enable measurements of macroalgal specimens and analyse densities. Video was converted into stills using frame-grabbing procedures and subsequently stitched together using the software Agisoft Metashape®. Ortho-mosaics were scaled using parallel lasers at six points evenly distributed along the transects. Both high-resolution still imagery and lower-resolution stitched imagery were used for further taxonomic identification of macroalgal species alongside collections.

Specimen collections

During the 2023 voyage, macroalgal specimens were recorded from several locations. Benthic samples were taken using a Van Veen Grab (0.13 m²) and an Agassiz Sled (1.15 m × 0.37 m). Samples were collected from Robertson Bay, Cape Adare, and the Possession Islands. These specimens were used to

confirm species identification from imagery. Reference specimens were created, including samples for genetic sequencing. Voucher specimens have been deposited in the Herbarium of the Museum of New Zealand Te Papa Tongarewa (WELT—Thiers 2023).

Benthic light availability and primary productivity modelling

Alongside in situ surveys of macroalgal communities, we used global modelling of sea-floor light⁴⁶ to estimate photosynthetically active radiation (PAR) reaching the seafloor. We used the R-package “coastalLight”⁴⁵ to examine light quantity across the Ross Sea region. This package combines global bathymetric models, radiation at the sea surface and metrics for light attenuation through the water column to calculate the irradiance at the seabed. However, challenges in determining key water clarity metrics (e.g., the light attenuation coefficient K_d) greatly impact the retrieval of EBed in the Antarctic region. To accommodate this, we further estimate EBed for regions where K_d measures were unavailable by replacing missing values with regional averages of K_d using the formula¹, which calculated light at the seabed using irradiance at the surface (I_s), and water depth (d).

$$EBed = I_s(e^{K_d \cdot d}) \quad (1)$$

Using the “coastalLight” package we explored light at the seabed for each region where seabed imagery was collected. For each individual region, we examined light at the seabed (EBed) across three replicate transects intersecting the coordinates of stations where seafloor imagery was collected. Each transect was perpendicular to the shore, covering shallow water to depths > 100 m. Limitations in available bathymetric information affected the retrieval of EBed at depths shallower than 50 m for some locations.

We combined outputs from ref.⁴⁶ with published photosynthetic parameters for three major macroalgal species found in Antarctica (*H. grandifolius*, *P. decipiens*⁵⁰, and CCA⁵¹) to examine net primary productivity (NPP). Published literature was searched using the key terms ‘photosynthetic parameters’, ‘Antarctica’, ‘macroalgae’, and the species names to establish key species-specific parameters. The photosynthetic parameters a (light use efficiency), R (respiration rate), and P_m (maximum productivity) were calculated for every cell where EBed was available, and the productivity (P) was calculated using the ref.⁸⁵ formula².

$$P = P_m \left(1 - e^{-\frac{a \cdot EBed}{P_m}} \right) + R \quad (2)$$

For every pixel (1/240 degree) in the wider Ross Sea region, we estimated the balance of NPP based on light at the seafloor (a function of PAR at the surface, water clarity and bathymetry). NPP was estimated at the lowest cell size as expressed by the bathymetric layer. Given the variability in PAR at the surface and water clarity (K_d), potential NPP values were identified across the Ross Sea region, and the modelled depth thresholds for each species are identified as defined by compensating irradiance (the light intensity at which respiration and primary productivity are balanced). All models and plots were run using the ‘R’ statistical software⁸⁶.

Estimates of carbon fixation

Estimates of Antarctic-wide macroalgal carbon fixation were estimated by extrapolating NPP across the estimated latitudinal range for each of the three modelled species (i.e., *H. grandifolius* between latitude 60–72.5°S, *P. decipiens* 60–75°S, and CCA 60–80°S). For every pixel (1/240°) with sufficient benthic light above compensating irradiance (i.e., NPP > 0), the net carbon fixation rate was calculated using photosynthetic parameters^{50–52} and the productivity–irradiance equation² and converted to monthly carbon fixed (kg). Values were then multiplied by cell area and summed across two regions, (1) the Ross Sea region (longitudes 160–172.5°) and (2) the Antarctic region (longitudes –180° to 180°). Latitudes of the two regions were defined by the observed range for each species. The summed NPP was then corrected for one standard deviation on each side of the mean coverage of

macroalgae across all transects shallower than 90 m. Mean coverage of macroalgae ranged from 6.6% (*P. decipiens*), 4.3% (*H. grandifolius*), and 1.4% (CCA). Total NPP was further adjusted to account for regions of suitable substrata (estimated as 30% of total area¹⁵) and limited growing seasons (5 months of sufficient light). These values were then compared to global estimates of macroalgal carbon fixation identified by Duarte et al.¹⁵ as ca. 1.32 pg C/year.

Reporting summary

Further information on research design is available in the Nature Portfolio Reporting Summary linked to this article.

Data availability

The datasets generated during and/or analysed during the current study are available in the online database Dryad <https://doi.org/10.5061/dryad.w6m905qgwz>. Data used in this study consist of abundance and density counts of macroalgae extracted from video transects; these data are available as tables and data-frames. Metadata for study sites is also provided in table form. Modelled outputs presented here can be generated using the R-package “coastalLight”.

Received: 16 October 2023; Accepted: 2 April 2024;

Published online: 17 April 2024

References

- Krause-Jensen, D. & Duarte, C. M. Substantial role of macroalgae in marine carbon sequestration. *Nat. Geosci.* **9**, 737–742 (2016).
- Krause-Jensen, D. et al. Sequestration of macroalgal carbon: the elephant in the Blue Carbon room. *Biol. Lett.* **14**, 20180236 (2018).
- Macreadie, P. I. et al. The future of Blue Carbon science. *Nat. Commun.* **10**, 1–13 (2019).
- Ortega, A. et al. Important contribution of macroalgae to oceanic carbon sequestration. *Nat. Geosci.* **12**, 748–754 (2019).
- Pessarrodona, A. et al. Carbon sequestration and climate change mitigation using macroalgae: a state of knowledge review. *Biol. Rev.* <https://doi.org/10.1111/brv.12990> (2023).
- Nielsen, S. L., Banta, G. T. & Pedersen, M. F. Decomposition of marine primary producers: consequences for nutrient recycling and retention in coastal ecosystems. In *Estuarine Nutrient Cycling: The Influence of Primary Producers*, (eds. Nielsen, S. L., Banta, G. & Pedersen, M. F.) 187–216, 303 (Kluwer Academic Publishers, Netherlands, 2004).
- Filbee-Dexter, K. et al. Kelp carbon sink potential decreases with warming due to accelerating decomposition. *PLoS Biol.* **20**, e3001702 (2022).
- Krause-Jensen, D. & Duarte, C. M. Expansion of vegetated coastal ecosystems in the future Arctic. *Front. Mar. Sci.* **1**, 77 (2014).
- Bellgrove, A. et al. Patterns and drivers of macroalgal ‘blue carbon’ transport and deposition in near-shore coastal environments. *Sci. Total Environ.* **890**, 164430 (2023).
- Attard, K. et al. Seafloor primary production in a changing Arctic Ocean. *Proc. Natl Acad. Sci. USA* **121**, e2303366121 (2024).
- Braeckman, U. et al. Degradation of macroalgal detritus in shallow coastal Antarctic sediments. *Limnol. Oceanogr.* **64**, 1423–1441 (2019).
- Küpper, F. C. et al. Juvenile morphology of the large Antarctic canopy-forming brown alga, *Desmarestia menziesii* J. Agardh. *Polar Biol.* **42**, 2097–2103 (2019).
- Deregis, D. et al. Carbon balance under a changing light environment. In: *Antarctic Seaweeds: Diversity, Adaptation and Ecosystem Services* (eds. Gómez, I. & Huovionen, P.) 3–20, 397 (Springer, Berlin, Heidelberg, 2020).
- Morley, S. A. et al. Benthic biodiversity, carbon storage and the potential for increasing negative feedbacks on climate change in shallow waters of the Antarctic Peninsula. *Biology* **11**, 320 (2022).

15. Duarte, C. M. et al. Global estimates of the extent and production of macroalgal forests. *Global Ecol. Biogeogr.* **31**, 1422–1439 (2022).
16. Wiencke, C., Amsler, C. D. & Clayton, M. N. Macroalgae. In *Biogeographic Atlas of the Southern Ocean* (eds. De Broyer, C. & Koubbi, P.) 66–73 (Scientific Committee on Antarctic Research, 2014).
17. Wiencke, C. & Amsler, C. D. Seaweeds and their communities in polar regions. In *Seaweed Biology: Novel Insights Into Ecophysiology, Ecology and Utilization* (eds. Wiencke, C. & Bischof, K.) 265–291 (Springer, Berlin, Heidelberg, 2012).
18. Amsler, C. D., Rowley, R. J., Laur, D. R., Quetin, L. B. & Ross, R. M. Vertical distribution of Antarctic peninsular macroalgae: cover, biomass and species composition. *Phycologia* **34**, 424–430 (1995).
19. Valdivia, N., Díaz, M. J., Garrido, I. & Gómez, I. Consistent richness-biomass relationship across environmental gradients in a marine macroalgal-dominated subtidal community on the western Antarctic Peninsula. *PLoS ONE* **10**, e0138582 (2015).
20. Quartino, M. L. et al. Production and biomass of seaweeds in newly ice-free areas: implications for coastal processes in a changing Antarctic environment. In *Antarctic Seaweeds: Diversity, Adaptation and Ecosystem Services* (eds. Gómez, I. & Huovionen, P.) 155–171, 397 (Springer, Berlin, Heidelberg, 2020).
21. Hop, H., Wiencke, C., Vögele, B. & Kovaltchouk, N. A. Species composition, zonation, and biomass of marine benthic macroalgae in Kongsfjorden, Svalbard. *Bot. Mar.* **55**, 399–414 (2012).
22. Paar, M. et al. Temporal shift in biomass and production of macrozoobenthos in the macroalgal belt at Hansneset, Kongsfjorden, after 15 years. *Polar Biol.* **39**, 2065–2076 (2016).
23. Reed, D. C., Rassweiler, A. & Arkema, K. K. Biomass rather than growth rate determines variation in net primary production by giant kelp. *Ecology* **89**, 2493–2505 (2008).
24. Desmond, M. J., Pritchard, D. W. & Hepburn, C. D. Light limitation within southern New Zealand kelp forest communities. *PLoS ONE* **10**, e0123676 (2015).
25. Smith, K. E., Moore, P. J., King, N. G. & Smale, D. A. Examining the influence of regional-scale variability in temperature and light availability on the depth distribution of subtidal kelp forests. *Limnol. Oceanogr.* **67**, 314–328 (2022).
26. Dayton, P. K. Competition, disturbance, and community organization: the provision and subsequent utilization of space in a rocky intertidal community. *Ecol. Monogr.* **41**, 351–389 (1971).
27. Dieckmann, G., Reichardt, W. & Zieliński, K. Growth and production of the seaweed, *Himantothallus grandifolius*, at King George Island. In *Antarctic Nutrient Cycles and Food Webs* (eds. Siegfried, W. R., Condy, P. R. & Laws, R. M.) 104–108 (Springer, Berlin, Heidelberg, 1985).
28. Amsler, C. et al. Gastropod assemblages associated with *Himantothallus grandifolius*, *Sarcopeltis antarctica* and other subtidal macroalgae. *Antarct. Sci.* **34**, 246–255 (2022).
29. Krumhansl, K. A. & Scheibling, R. E. Production and fate of kelp detritus. *Mar. Ecol. Prog. Ser.* **467**, 281–302 (2012).
30. Renaud, P. E., Løkken, T. S., Jørgensen, L. L., Berge, J. & Johnson, B. J. Macroalgal detritus and food-web subsidies along an Arctic fjord depth-gradient. *Front. Mar. Sci.* **2**, 31 (2015).
31. Reichardt, W. T. Burial of Antarctic macroalgal debris in bioturbated deep-sea sediments. *Deep Sea Res. Part A Oceanogr. Res. Pap.* **34**, 1761–1770 (1987).
32. Cook, A. J., Fox, A. J., Vaughan, D. G. & Ferrigno, J. G. Retreating glacier fronts on the Antarctic Peninsula over the past half-century. *Science* **308**, 541–544 (2005).
33. Milillo, P. et al. Rapid glacier retreat rates observed in West Antarctica. *Nat. Geosci.* **15**, 48–53 (2022).
34. Mezzina, B., Goosse, H., Klein, F., Barthélemy, A. & Massonnet, F. Atmospheric drivers of Antarctic sea ice extent summer minima. *Cryosphere Discuss.* **2023**, 1–20 (2023).
35. Wang, S. et al. Contribution of the deepened Amundsen Sea low to the record low Antarctic sea ice extent in February 2022. *Environ. Res. Lett.* **18**, 054002 (2023).
36. Purich, A. & Doddridge, E. W. Record low Antarctic sea ice coverage indicates a new sea ice state. *Commun. Earth Environ.* **4**, 314 (2023).
37. Sahade, R. et al. Climate change and glacier retreat drive shifts in an Antarctic benthic ecosystem. *Sci. Adv.* **1**, e1500050 (2015).
38. Amsler, C. D. et al. Strong correlations of sea ice cover with macroalgal cover along the Antarctic Peninsula: ramifications for present and future benthic communities. *Elem. Sci. Anthr.* **11**, 20 (2023).
39. Zwerschke, N. et al. Quantification of blue carbon pathways contributing to negative feedback on climate change following glacier retreat in West Antarctic fjords. *Global Change Biol.* **28**, 8–20 (2022).
40. Deregibus, D. et al. Photosynthetic light requirements and vertical distribution of macroalgae in newly ice-free areas in Potter Cove, South Shetland Islands, Antarctica. *Polar Biol.* **39**, 153–166 (2016).
41. Barnes, D. K. et al. Societal importance of Antarctic negative feedbacks on climate change: blue carbon gains from sea ice, ice shelf and glacier losses. *Sci. Nat.* **108**, 1–14 (2021).
42. Deregibus, D. et al. Potential macroalgal expansion and blue carbon gains with northern Antarctic Peninsula glacial retreat. *Mar. Environ. Res.* **189**, 106056 (2023).
43. Barnes, D. K., Fleming, A., Sands, C. J., Quartino, M. L. & Deregibus, D. Icebergs, sea ice, blue carbon and Antarctic climate feedbacks. *Philos. Trans. R. Soc. A* **376**, 20170176 (2018).
44. Barnes, D. K. Iceberg killing fields limit huge potential for benthic blue carbon in Antarctic shallows. *Global Change Biol.* **23**, 2649–2659 (2017).
45. Field, C. B., Behrenfeld, M. J., Randerson, J. T. & Falkowski, P. Primary production of the biosphere: integrating terrestrial and oceanic components. *Science* **281**, 237–240 (1998).
46. Gattuso, J. P., Gentili, B., Antoine, D. & Doxaran, D. Global distribution of photosynthetically available radiation on the seafloor. *Earth Syst. Sci. Data* **12**, 1697–1709 (2020).
47. Thoralf, F., Pinkerton, M. H., Tait, L. W. & Schiel, D. R. Spectral light quality on the seabed matters for macroalgal community composition at the extremities of light limitation. *Limnol. Oceanogr.* **68**, 902–916 (2023).
48. Wulff, A. et al. Biodiversity, biogeography and zonation of marine benthic micro- and macroalgae in the Arctic and Antarctic. *Bot. Marina* **52**, 491–507 (2009).
49. Robinson, B. J. O. et al. New confirmed depth limit of Antarctic macroalgae: *Palmaria decipiens* found at 100 m depth in the Southern Ocean. *Polar Biol.* **45**, 1459–1463 (2022).
50. Quartino, M., KloEser, H., Schloss, I. & Wiencke, C. Biomass and associations of benthic marine macroalgae from the inner Potter Cove (King George Island, Antarctica) related to depth and substrate. *Polar Biol.* **24**, 349–355 (2001).
51. Gomez, I., Weykam, G., Klöser, H. & Wiencke, C. Photosynthetic light requirements, metabolic carbon balance and zonation of sublittoral macroalgae from King George Island (Antarctica). *Mar. Ecol. Prog. Ser.* **148**, 281–293 (1997).
52. Schwarz, A. M. et al. Primary production potential of non-geniculate coralline algae at Cape Evans, Ross Sea, Antarctica. *Mar. Ecol. Prog. Ser.* **294**, 131–140 (2005).
53. Zaneveld, J. S. The occurrence of benthic marine algae under shore fast-ice in the western Ross Sea, Antarctica. In *Proc. International Seaweed Symposium* (eds. Young, E. D. & McLachlan, J. L.) Vol. **5**, 217–231 (Pergamon Press, Oxford, 1966).
54. Zaneveld, J. S. Benthic marine algae, Ross Island to the Balleny Islands. *Antarctic Map Folio Series* 10: 10–12, 13 (Am Geograph Soc., New York, 1968).

55. Cummings, V., Thrush, S., Schwarz, A. M., Funnell, G. & Budd, R. *Ecology of Coastal Benthic Communities of the North Western Ross Sea*. Aquatic Biodiversity and Biosecurity Report for Ministry of Fisheries Research Project ZBD2003/02. New Zealand Aquatic Environment and Biodiversity Report, no. 6, 67 (NIWA, New Zealand, Wellington, 2005).
56. Nelson, W. A., Neill, K. F., D'Archino, R. & Sutherland, J. E. Marine macroalgae of the Balleny Islands and Ross Sea. *Antarct. Sci.* **34**, 298–312 (2022).
57. Thrush, S. et al. Broad-scale factors influencing the biodiversity of coastal benthic communities of the Ross Sea. *Deep Sea Res. Part II: Top. Stud. Oceanogr.* **53**, 959–971 (2006).
58. Cummings, V. J., Thrush, S. F., Chiantore, M., Hewitt, J. E. & Cattaneo-Vietti, R. Macrobenthic communities of the north-western Ross Sea shelf: links to depth, sediment characteristics and latitude. *Antarct. Sci.* **22**, 793–804 (2010).
59. Nelson, W. et al. Beyond diving depths: deepwater macroalgae in the New Zealand region. *Mar. Biodivers.* **45**, 797–818 (2015).
60. Tait, L. et al. Deep-living and diverse Antarctic seaweeds are potentially important contributors to global carbon fixation [Dataset]. *Dryad*. <https://doi.org/10.5061/dryad.w6m905qwz> (2024).
61. Pessarrodona, A. et al. A global dataset of seaweed net primary productivity. *Sci. Data* **9**, 484 (2022).
62. Siegert, M. J. et al. Antarctic extreme events. *Front. Environ. Sci.* **11**, 1229283 (2023).
63. Wiencke, C. Seasonality of brown macroalgae from Antarctica—a long-term culture study under fluctuating Antarctic daylengths. *Polar Biol.* **10**, 589–600 (1990a).
64. Wiencke, C. Seasonality of red and green macroalgae from Antarctica—a long-term culture study under fluctuating Antarctic daylengths. *Polar Biol.* **10**, 601–607 (1990b).
65. Zieliński, K. Bottom macroalgae of the Admiralty Bay (King George Island, South Shetlands, Antarctica). *Pol. Polar Res.* **11**, 95–131 (1990).
66. Wiencke, C., Amsler, C. D., Clayton, M. N. & Van de Putte, A. *SCAR Biogeographic Atlas of the Southern Ocean—Macroalgae—Data*. Antarctic Biodiversity Information Facility (ANTABIF) <https://doi.org/10.15468/tybssc> (2020).
67. Krause-Jensen, D. et al. Seasonal sea ice cover as principal driver of spatial and temporal variation in depth extension and annual production of kelp in Greenland. *Global Change Biol.* **18**, 2981–2994 (2012).
68. Castro de la Guardia, L. et al. Increasing depth distribution of Arctic kelp with increasing number of open water days with light. *Elem. Sci. Anthr.* **11**, 00051 (2023).
69. Krause-Jensen, D. et al. Deep penetration of kelps offshore along the west coast of Greenland. *Front. Mar. Sci.* **6**, 375 (2019).
70. Schimani, K. et al. Video survey of deep benthic macroalgae and macroalgal detritus along a glacial Arctic fjord: Kongsfjorden (Spitsbergen). *Polar Biol.* **45**, 1291–1305 (2022).
71. Clark, G. F. et al. Light-driven tipping points in polar ecosystems. *Global Change Biol.* **19**, 3749–3761 (2013).
72. Pellizzari, F. et al. Diversity and spatial distribution of seaweeds in the South Shetland Islands, Antarctica: an updated database for environmental monitoring under climate change scenarios. *Polar Biol.* **40**, 1671–1685 (2017).
73. Oliveira, M. C., Pellizzari, F., Medeiros, A. S. & Yokoya, N. S. Diversity of Antarctic seaweeds. In *Antarctic Seaweeds: Diversity, Adaptation and Ecosystem Services* (eds. Gómez, I. & Huovionen, P.) 23–42 (Springer, Berlin, Heidelberg, 2020).
74. Pellizzari, F. et al. New records and updated distributional patterns of macroalgae from the South Shetland Islands and northern Weddell Sea, Antarctica. *Antarct. Sci.* **35**, 243–255 (2023).
75. Long, M. C. et al. Strong Southern Ocean carbon uptake evident in airborne observations. *Science* **374**, 1275–1280 (2021).
76. Arrigo, K. R. et al. Phytoplankton community structure and the drawdown of nutrients and CO₂ in the Southern Ocean. *Science* **283**, 365–367 (1999).
77. Arteaga, L. A., Boss, E., Behrenfeld, M. J., Westberry, T. K. & Sarmiento, J. L. Seasonal modulation of phytoplankton biomass in the Southern Ocean. *Nat. Commun.* **11**, 5364 (2020).
78. Lohrer, A. M., Cummings, V. J. & Thrush, S. F. Altered sea ice thickness and permanence affects benthic ecosystem functioning in coastal Antarctica. *Ecosystems* **16**, 224–236 (2013).
79. CCAMLR. *Conservation Measure 91-05 (2016): Ross Sea Region Marine Protected Area*. 1–17 (CCAMLR, Hobart, Australia, 2016).
80. Epstein, G., Middelburg, J. J., Hawkins, J. P., Norris, C. R. & Roberts, C. M. The impact of mobile demersal fishing on carbon storage in seabed sediments. *Global Change Biol.* **28**, 2875–2894 (2022).
81. Arafah-Dalmau, N. et al. Southward decrease in the protection of persistent giant kelp forests in the northeast Pacific. *Commun. Earth Environ.* **2**, 119 (2021).
82. Bowden, D. A., Schiaparelli, S., Clark, M. R. & Rickard, G. J. A lost world? Archaic crinoid-dominated assemblages on an Antarctic seamount. *Deep Sea Res. Part II: Top. Stud. Oceanogr.* **58**, 119–127 (2011).
83. Althaus, F. et al. A standardised vocabulary for identifying benthic biota and substrata from underwater imagery: the CATAMI classification scheme. *PLoS ONE* **10**, e0141039 (2015).
84. Bowden, D. A. et al. *Best Practice in Seabed Image Analysis for Determining Taxa, Habitat, or Substrata Distributions*. New Zealand Aquatic Environment and Biodiversity Report No. 239 61 (Ministry of Primary Industries, Wellington, N.Z., 2020) <https://doi.org/10.25607/OBP-1908>.
85. Jassby, A. D. & Platt, T. Mathematical formulation of the relationship between photosynthesis and light for phytoplankton. *Limnol. Oceanogr.* **21**, 540–547 (1976).
86. R Core Team. *R: A Language and Environment for Statistical Computing* (R Foundation for Statistical Computing, Vienna, Austria, 2022).

Acknowledgements

We thank the crew of the Research Vessel RV *Tangaroa* for their skill and diligence in allowing us to access and navigate the shallow coastal waters of the Ross Sea in 2021 and 2023. We thank Dr. Joshu Mountjoy, voyage leader for the 2023 survey, and the science crew that contributed to this work across both voyages. In particular, we thank Arne Pallentin, Dr. Yoann Lacroix, and Dr. Erica Spain for operating the multi-beam echosounders onboard RV *Tangaroa* while accessing shallow water locations. We thank the New Zealand Ministry of Foreign Affairs and Trade for reviewing and approving our activities in the Ross Sea Region. We acknowledge the New Zealand Antarctic Science Platform (ASP), the New Zealand Ministry for Business Innovation and Employment (MBIE ANTA1801), and the National Institute of Water and Atmospheric Research's Coasts and Estuaries Strategic Science Investment Fund for funding.

Author contributions

L.W.T., C.C., P.M., S.G., R.L.O., M.L., and V.S.M. contributed to voyage surveys, L.W.T., C.C., and W.N. analysed and processed video data from the voyage, L.W.T. performed modelling of seabed light and primary productivity, L.W.T., W.N., and V.J.C. drafted the manuscript, L.W.T., V.J.C., and M.L. conceived the research, and all authors contributed to the final draft manuscript.

Competing interests

The authors declare no competing interests.

Additional information

Supplementary information The online version contains supplementary material available at <https://doi.org/10.1038/s43247-024-01362-2>.

Correspondence and requests for materials should be addressed to Leigh W. Tait.

Peer review information *Communications Earth & Environment* thanks Charles Amsler and Franciane Pellizzari for their contribution to the peer review of this work. Primary Handling Editors: Clare Davis. A peer review file is available.

Reprints and permissions information is available at <http://www.nature.com/reprints>

Publisher's note Springer Nature remains neutral with regard to jurisdictional claims in published maps and institutional affiliations.

Open Access This article is licensed under a Creative Commons Attribution 4.0 International License, which permits use, sharing, adaptation, distribution and reproduction in any medium or format, as long as you give appropriate credit to the original author(s) and the source, provide a link to the Creative Commons licence, and indicate if changes were made. The images or other third party material in this article are included in the article's Creative Commons licence, unless indicated otherwise in a credit line to the material. If material is not included in the article's Creative Commons licence and your intended use is not permitted by statutory regulation or exceeds the permitted use, you will need to obtain permission directly from the copyright holder. To view a copy of this licence, visit <http://creativecommons.org/licenses/by/4.0/>.

© The Author(s) 2024